

1 storage zone of the SGSP reached approximately 90 °C. The overall performance was evaluated
2 in two periods (2014 and 2015) in terms of the retrofitting of mining facility with a solar pond and a
3 new method to assess the thermal efficiency of the solar pond in a long-term perspective has
4 been proposed. The overall efficiencies obtained after the first and second operation periods
5 were 10 and 12%, respectively, with maximum values of 28 and 24% obtained during the first
6 operation months. Regarding the economic savings, the fuel oil cost of the flotation unit was
7 reduced by a higher percentage than the fuel oil consumption, due to the decreasing tendency of
8 fuel oil prices during 2014 and 2015. Reductions of 52 and 68% were obtained in the first and
9 second periods of operation, respectively, when compared to 2013. In addition, not only does the
10 SGSP have considerably reduced operating costs but also the environmental costs are clearly
11 reduced when considering the reduction of CO₂ emissions.

12
13 Keywords: solar energy; heat extraction; renewable energy; energy efficiency; mineral flotation.

14 15 **1. Introduction**

16 The emission of greenhouse gases and their impact on climate change are of major concern
17 nowadays. Solar energy is promoted as one of the most promising substitutes for traditional
18 energy resources; however, its intermittent and unstable nature is a major drawback, which leads
19 to a disparity between supply and demand (Valderrama et al., 2016; Yu et al., 2013).

20
21 Solar ponds are classified into the category of a solar thermal system, functioning as both a
22 collector and a storage facility of solar energy for future use. Solar ponds have been investigated
23 extensively over the past decades. The characteristics that make them attractive are, first, the
24 capacity for long-term storage, which can supply sufficient heat for the entire year, and second,
25 the annual collection efficiency in the range of 15–25% for all locations and the capacity to supply

adequate heat even at higher latitudes. A solar pond consists of three distinct zones. The first is located at the top of the pond and contains the less dense salt/water mixture; this is the upper convective zone (UCZ), which has the function of protecting the salinity-gradient layer. In the second zone, the salt/water density varies, increasing with depth; this is the gradient zone or non-convective zone (NCZ), also called the salinity-gradient layer. The main purpose of this zone is to act as an insulator to prevent heat from escaping to the UCZ, thus maintaining higher temperatures in the deeper zones. The third zone is the lower convective zone (LCZ), also called the energy storage zone, which consists of saturated brine with almost homogeneous salinity and density. The heat stored in the LCZ can be used as a heat source for the heating of buildings, power production, and industrial processing (L. C. Ding et al., 2016) or can be utilized to drive a turbine for electric power generation by means of an organic refrigerant (L.C. Ding et al., 2016). Solar ponds have been studied around the world for more than half a century and successful case studies have been reported (Table 1) in Israel, the USA, India, China, Australia, and Spain.

Table 1. Successful experimental solar ponds reported in the literature during the last 5 decades.

		Name/Site	Construction year	Area (m ²)	Maximum temperature (LCZ)	Applications	References
Israel	Eilat	Ein Boqek solar pond	1977	6250	85-90	Electrical production	(Tabor and Doron, 1986)
		Beith Ha'rava solar pond	1982	25000		Electrical production	(Tabor and Doron, 1990)
USA	Ohio	Ohio State University		200	62-69	Pilot Plant (research)	(Rabl and Nielsen, 1975)
		Ohio State University		400		Pilot Plant (research)	(Nielsen, 1980)
		Ohio Agricultural Research and Development Centre	1977	156	46	Heating building (Greenhouse)	(Fynn, 1981)
		Miamisburg	1978	2020	51.1	Heating building (Swimming pool and recreational building)	(Shah et al., 1981; Bryant et al., 1979)
	New Mexico	University of New Mexico (Albuquerque)	1975	175	93	Heating building (House)	(Wilkins et al., 1986; Zangrando, 1991)
	Texas	University of Texas (El Paso)	1983	3355	72	Industrial process heat (food canning factory); Desalination, electrical power production	(Reid et al., 1985; Swift et al., 1987; Liao et al., 1988; Hull and Nielsen, 1988)
	Illinois	University of Illinois	1987	2000	70	Heating building (swine research)	(Newell et al., 1990)

						facility)	
India	Bhavnagar	Central Salt and Marine Chemicals Research Inst.	1970	1200		Pilot Plant (research)	(Srinivasan, 1993)
		Institute's experimental salt farm	1980	1600	75	Pilot Plant (research)	(Mehta et al., 1988)
	Bangalore	Institute of science in Bangalore (Pondicherry)		100	70	Pilot Plant (research)	(Patel and Gupta, 1981)
		Indian Institute of Science	1984	240	50-70	Pilot Plant (research)	(Srinivasan, 1990; Akbarzadeh and Manins, 1988)
	Karnataka	Masur		400		Heating building (Rural community)	(Srinivasan, 1993)
		Hubli		300		Heating building (To supply hot water for college)	
	Gujerat	Khuj Dairy (Bhuj)	1987-1991	6000	99.8	Industrial process heat (Milk processing dairy plant)	(Kumar and Kishore, 1999)
Australia	Aspendale (Victoria)	Commonwealth Scientific and Industrial Res. Org.	1964	44	63	Pilot Plant (research)	(Davey, 1968)
	Laverton (Victoria)	Cheetham Salt Works	1981	900		Pilot Plant (research)	(Golding et al., 1982)
	Alice Spring	Northern Territory	1980	2000	80	Electrical power production	(Collins, 1984)
			1984	1600	80-85	Electrical power production	(Sherman and Imberger, 1991)
	Pyramid Hill (Victoria)	Pyramid Salt Ltd facility/ RMTI University	2000	3000	62	Industrial process heat	(Leblanc et al., 2011)
Other countries	Argentina	Puna	1981	400		Chemical production	(Lesino et al., 1990; Lesino and Saravia, 1991)
	Italy	Margherita Di Savoia		25000		Desalination	(Folchitto, 1997)
	China	Zabuya Lake (Qinghai Tibet Plateau)		2500	39	Chemical production	(Nie et al., 2011)
	Spain	Solvay Martorell (Catalonia)	2009	50	63	Pilot Plant (research)	(Valderrama et al., 2011; Bernad et al., 2013; Alcaraz et al., 2016)

1

2 Recently, several studies have been conducted experimentally and numerically to analyse the
3 performance of solar ponds and understand their functional mechanisms. The experimental
4 studies have been focused on i) exploring alternative applications e.g., the combination of
5 membrane distillation with solar ponds (Rahaoui et al., 2017), the thermophilic digestion of waste-

1 activated sludge coupled with a solar pond (Zhang et al., 2016); ii) the addition of heat to solar
2 pond from external sources (Ganguly et al., 2017); iii) the analysis of solar pond performance and
3 monitoring to improve the overall efficiency (Sayer et al., 2108; Simic and George, 2017;
4 A.A.Abdullah et al., 2017; Torkmahalleh et al., 2107; Bozkurt and Karakilcik, 2015a); and iv) the
5 energy and exergy efficiencies analysis (Njoku et al., 2017; Khalilian, 2017a, 2017b; Bozkurt and
6 Karakilcik, 2015b). Contrary, scarce examples of industrial solar ponds can be found.

7 The aim of this paper is to describe the design, construction, and operation of a 500 m² industrial
8 solar pond in Granada (Spain). This solar pond was constructed with the purpose of delivering a
9 heat stream of up to 60 °C to minimize the fuel oil consumption at the mineral processing facility.

10 The overall performance of the solar pond was evaluated during two periods (2014 and 2015)
11 and the solar pond efficiency was assessed in terms of the integration of the solar pond with the
12 flotation unit of the mining facility. Finally, an economic analysis is also presented in terms of the
13 savings in fossil fuel consumption and reduction of greenhouse gas emissions.

14
15 **2. Description of the solar pond**

16 **2.1 Pond specifications and site arrangement**

17 The Granada Solar Pond is a collaborative project between Barcelona Tech UPC, RMIT
18 University, and Solvay Energy Service to study this solar technology as a new energy system
19 capable of capturing and storing solar energy and using this energy as a low thermal application
20 in a mining facility located in Granada (south Spain). The purpose of this solar pond is to deliver
21 the heat required to preheat the water (> 60 °C) and the reagents in the mineral flotation unit.
22 Fuel oil was used for this purpose, and thus the installation of the SGSP offers significant benefits
23 by reducing fuel oil consumption and minimizing its environmental impact, which is mainly
24 associated with the greenhouse gas emissions. In 2014, an industrial salinity-gradient solar pond
25 (SGSP) was constructed in Solvay Minerales in Granada (south Spain). This solar pond was the

1 first industrial solar pond in Europe. The total area of the pond is 500 m² (20 × 25 m) and it has a
 2 depth of 2.2 m. Table 2 shows the main climatological parameters of the solar pond's location
 3 (Bernad et al., 2013). The LCZ was designed to be 0.6 m thick, the NCZ was 1.4 m thick, and the
 4 UCZ was 0.2 m thick.
 5 Table 2. Location and climatological parameters at Solvay Minerales mining facilities in Granada
 6 (Spain) (values correspond to the data from 2014).

Coordinates										37° 3' 0" N, 3° 45' 0" W		
Altitude (m)										929		
Wind average speed (m/s)										2.3		
Summer maximum temperature (°C)										33.0		
Winter minimum temperature (°C)										-7.0		
	January	February	March	April	May	June	July	August	September	October	November	December
Average ambient temperature (°C)	3.10	4.20	7.30	10.0	13.3	18.1	21.9	21.4	18.1	12.0	7.2	4.1
Solar radiation (MJ/m ² month)	283	346	496	618	734	813	838	748	565	400	275	227

2.2 Insulation and lining materials

9 The bottom and the walls were insulated using a synthetic insulation material, ChovAFOAM 300-
 10 M50 (thermal conductivity = 0.034 W/mK; thickness = 50 mm; maximum pressure = 300 kPa;
 11 maximum temperature = 65 °C) in order to prevent heat losses. Expanded clay pellets (Arlita)
 12 were laid on the base of the pond to a total height of 50 mm. This ensures that the insulation is
 13 well protected from the higher temperatures during summer time in the LCZ. The remainder of the
 14 wall, not covered with Arlita, was laid with a geotextile (non-woven polyester GTXnw PS NTL,
 15 Atarfil, Spain) in order to prevent contact between the ChovAFOAM 300-M50 insulation and the
 16 PVC liner (thickness of geotextile and PVC liner = 1 mm), so that they would not react with each

1 other. In addition, a secondary (PE) liner was used to prevent leakage in the system (thickness =
2 2 mm). Details of the base and wall insulation scheme of the solar pond are shown in Figure 1.



4 Figure 1. Insulation and lining of the Granada solar pond: details of installation of materials and
5 final configuration.

7 2.3 Heat extraction system

8 The heat extraction system is composed of one heat exchanger located at the LCZ. This heat
9 exchanger was built by using PE pipe with an internal diameter of 28 mm, an external diameter of
10 32 mm, and a thermal conductivity of approximately 0.33 W/(m.K). The total length is 1200 m,
11 which is divided into six independent spirals of 200 m, each installed in the bottom of the pond as
12 shown in Figure 2. Fixation of the exchangers to the bottom was carried out with the help of
13 concrete bricks.



1

2 Figure 2. Heat exchanger (1200 m in length) in the Granada solar pond, distributed in six
3 independent spirals of 200 m each. Fixation of the heat exchanger pipes was done by the use of
4 concrete bricks.

5

6 The aim of the study is to preheat the working fluid (water) to be used in the flotation unit of the
7 mining facility using the heat stored in the 500 m² solar pond. Two tanks of 5 m³ each are used to
8 feed the required reagents into the flotation unit, whose consumption is about 5 m³ in
9 approximately 16 hours. An alternate filling/emptying system is used for both tanks.
10 Independently of the flow rate, each tank is filled once a day, and thus 10 m³/day of warm water
11 (up to 60 °C) is used in the flotation unit. Depending on the flow rate, the duration of tank filling
12 varies. For this reason, the filling time of the tanks is calculated for different flow rates.

13 The solar pond was integrated with the flotation unit by connecting a pipe from the freshwater
14 tank that travels through the LCZ of the solar pond and joins the existing pipe line, as shown in
15 Figure S1 (Supplementary Material). When the solar pond is in use, the valve VFA is closed and
16 both valves VSA and VSB are open, allowing fresh water to enter and be heated by the solar
17 pond. Therefore, the solar pond heats the water reaching the flotation reagent tanks. If at any
18 time the solar pond cannot heat the water to the desired temperature, the existing boiler is used
19 (totally or partially) as if the flotation unit worked without the solar pond.

1

2 The optimal flow rate of heat exchanger was estimated in terms of the parameters listed in Table
3 3, assuming that the LCZ temperature is 50 °C and the temperature of the inlet tap water is 15
4 °C.

5 Table 3. Parameters used to estimate the optimal flow rate of the heat exchanger system.

LCZ temperature (°C)	50
Inlet cold water temperature (°C)	15
Flow rate (L/min)	0 –120
Heat exchanger length (m)	1200
Daily average solar radiation (MJ/m ²)	20
Daily volume fed to the flotation unit (L)	10000

6

7 The rate of thermal energy extracted from the solar pond is given by Eq. 1 (Leblanc et al., 2011):

$$Q = m \cdot C_p \cdot (T_o - T_i) \quad (1)$$

8 Where, Q (W) is the thermal energy extracted, m (kg/s) is mass flow rate, C_p (J/kg °C) is the
9 specific heat of water, T_o (°C) is the outlet temperature of the working fluid, and T_i (°C) is the inlet
10 temperature of the working fluid. Considering that the mineral flotation process needs 10000
11 L/day, the daily rate of thermal energy extracted for each flow rate can be calculated by Eq. 2:

$$q = Q \cdot t \quad (2)$$

12 Where, q (J) is the daily thermal energy extracted and t (s) is the daily time to fill the flotation
13 reagents tanks of 10000L capacity. The solar pond efficiency can be calculated by Eq. 3:

$$\eta = \frac{q}{A \cdot H} \quad (3)$$

14 Where, A (m²) is the area of the solar pond, H (J/m²) is the daily solar radiation at the surface of
15 the pond.

1 The efficiency for each flow rate (see Figure S2) varies between 17 and 12 %, which is a
2 reasonable value for salinity gradient solar pond performance.

3 The calculation performed indicated that a flow rate above 40 L/min leads to a decrease in the
4 efficiency of the heat exchanger and also a decrease in the outlet temperature of the working
5 fluid, as can be seen in Figures S2 and S3 (Supplementary Material). Then, a flow rate of 40
6 L/min was set for the heat exchanger to ensure that the required amount of warm water was fed
7 into the flotation unit.

9 **2.4 Monitoring and control of solar pond**

10 To control the stability of the salinity gradient, samples are taken every 10 cm from the bottom
11 area through a PVC pipe (6 mm in diameter with a height of 3 m) to determine the density, pH,
12 and turbidity of the system over its entire height. A DMA 35 portable density meter (Anton Par;
13 accuracy of $\pm 0.001 \text{ g/cm}^3$) is used to measure the density. The pH and turbidity are measured by
14 a portable pH meter (Crison pH25, accuracy of $\pm 0.01 \text{ pH}$) and a portable turbidity meter (Hanna
15 HI93703C, accuracy of $\pm 0.5 \text{ NTU}$), respectively. The temperature measurement at different
16 heights is performed by 42 sensors (thermo-resistances, PT100 type, Abco, Spain) uniformly
17 distributed at intervals of 5 cm, starting 0.5 cm from the bottom and installed in plastic supports.

18
19 The temperature is measured every 2 s and the average after 10 min as well as the hourly and
20 daily average is recorded. The monthly average temperature of each zone is determined by
21 averaging the values recorded daily. The weather parameters are measured by means of an
22 automatic weather station, the CR1000 Measurement and Control System (Campbell Scientific,

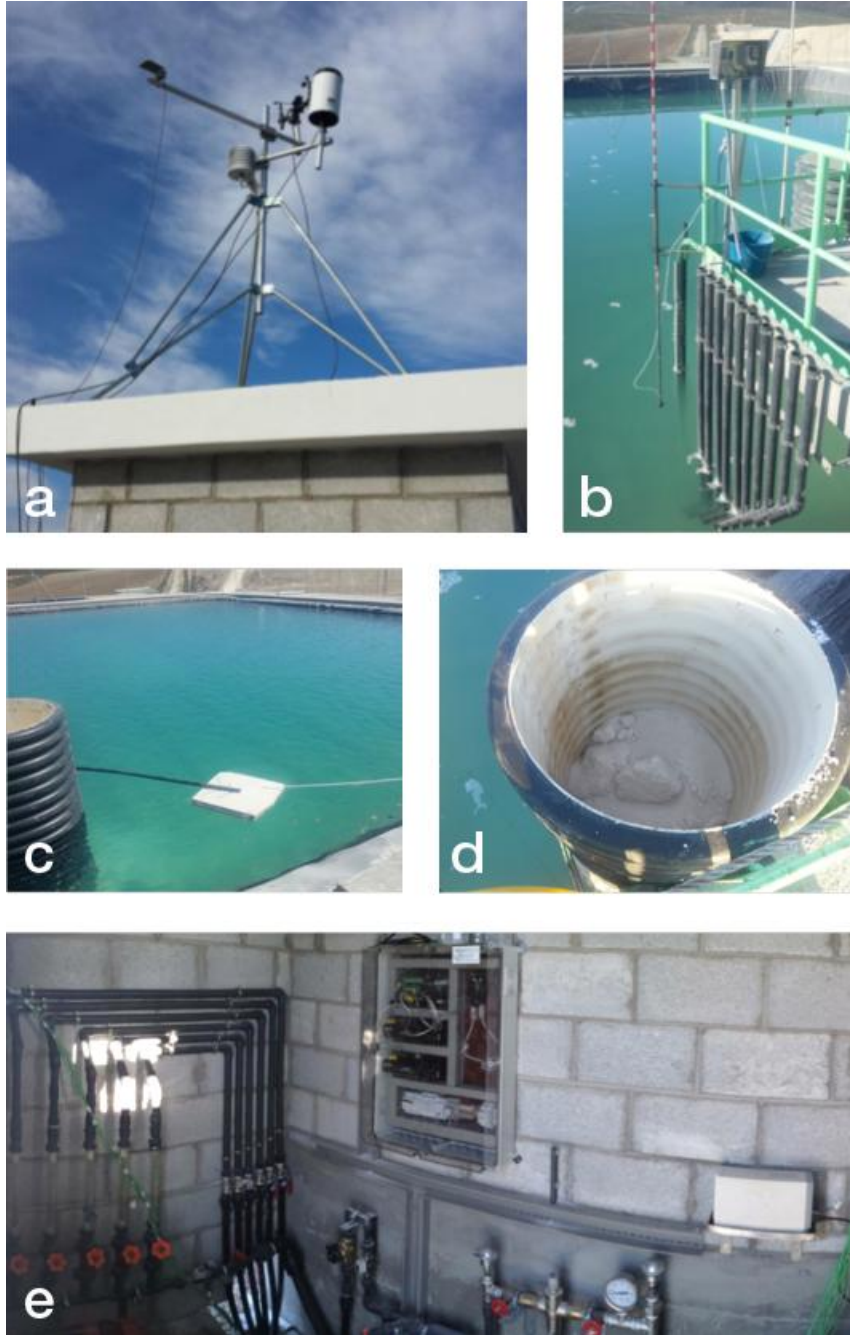


Figure 3. Monitoring and control systems at the Granada solar pond: a) weather station, b) acidification system, c) overflow system, d) salt charger, e) heat extraction monitoring.

Barcelona, Spain) (Figure 3a). The station was programmed to measure and store data (Datalogger CR1000) from the different meteorological sensors with high accuracy, as follows: rain (52202/52203, 2% up to 25 mm/h); solar radiation (CS300, $\pm 5\%$ for daily total radiation); wind speed (03002, ± 0.5 m/s); relative humidity (CS215, $\pm 2\%$, 10 to 90% RH); barometric

1 pressure (CS106, ± 0.6 mb, 0° to 40° C), and air temperature (CS215, $\pm 0.4^\circ$ C, over $+5$ to $+40$
2 $^\circ$ C). The sensors take measurements every 10 s, and the hourly average is recorded as well as
3 the daily average (24 h). The monthly average ambient temperature is determined by averaging
4 the values recorded daily.

5 Brine transparency is one of the most important factors affecting the solar pond performance,
6 along with the control of the pond level, to guarantee the stability of the gradient (NCZ). The level
7 of the water in the solar pond was fixed at 2.2 m above the bottom by using an overflow system.
8 Fresh water is added frequently at the surface to compensate for the evaporation losses and to
9 flush the surface using a pipe, 0.15 m in diameter, at a velocity of 1–3 L/min in order to avoid
10 causing disturbances on the surface and destabilizing the gradient (Figure 3c). To compensate
11 for the salt loss by diffusion, two salt chargers are employed to replenish the salt in the bottom
12 area to keep the concentration in this area constant. The chargers were made by using a PVC
13 cylinder with a diameter of 1.2 m and were fixed to the stairway (Figure 3d). Salt coming out of
14 the bottom of the cylinder produced a semi-cone around the charger. To control the clarity of the
15 system, an acidification system was installed to regulate the pH and to prevent the growth of
16 algae. The system to regulate the pH is composed of ten PVC pipes (Figure 3b). These tubes
17 have different lengths to allow the acid to be distributed in the different zones of the solar pond,
18 every 0.15 m from the LCZ–NCZ interface to the top. The acid (hydrochloric acid, 35% w/w) is
19 added into the system at a low velocity by a peristaltic pump in order to avoid disturbing the
20 system.

21 The sensors that control the process of heat extraction are located next to the solar pond in an
22 instrumentation room. The inlet and outlet temperatures of the working fluid are measured with
23 thermal sensors (PT100) and the total inlet flow rate is controlled by a flow meter (SMC) located
24 in the inlet and outlet pipes of the heat exchanger, as can be seen in Figure 3e. To ensure that
25 the inlet flow rate in each spiral was the same, a rotameter was installed in each of the individual

1 spiral heat exchangers. The working fluid circulates from a fresh water tank located 25 m from the
2 solar pond that runs by gravity, so a pump is not necessary. This flow is divided into the six
3 spirals located in the bottom area of the pond. The fresh water flows through the LCZ at a flow
4 rate between 20 and 40 L/ min, depending on the amount of warm water needed in the flotation
5 unit, and exits the pond at a temperature near to that of the storage zone. From there it goes to
6 the flotation unit located to 85 m from the solar pond (Figure S4, Supplementary Material). The
7 warm water goes to the application, taking advantage of the height difference between the solar
8 pond and the processing building.

10 **3. Results and discussion**

11 **3.1. Establishment of salinity gradient**

12 The key to the solar pond technology is the stability of the salinity gradient (NCZ). For this reason,
13 the establishment of the gradient zone is a critical task. During more than 25 years, several
14 studies describing the different techniques used to establish the salinity gradient have been
15 conducted, and as a result, water injection has become the most common and efficient method
16 (Hull et al., 1989; Liao, Y., Swift, A. & Golding, 1988; Valderrama et al., 2011; Zangrando, 1980).
17 This method was used to establish both the salinity and thermal gradients in the solar pond. First,
18 the pond is filled with saturated brine at a height of 1.32 m ($h_{LCZ} + \frac{1}{2} h_{NCZ}$), which corresponds to
19 a total volume of 662.5 m³. The necessary amount of brine is transported by trucks to the facility
20 simultaneously with the filling process. Then, the salinity gradient is settled by injecting low-
21 salinity water into the pond through a specially designed (Figure 4) and constructed diffuser, as
22 described elsewhere (Valderrama et al., 2011). The supporting vertical rod of the diffuser was
23 marked at intervals of 25 mm to find the distance between the plane of the diffuser and the water
24 level at any time to control the injection process.



1

2

3 Figure 4. Picture of the stainless steel diffuser used to establish the salinity gradient of the
 4 Granada solar pond. Diameter: 50 mm; gap width: 10 mm; thickness: 16 mm; pipe inlet diameter:
 5 50 mm.

6

7 The injection starts with the diffuser at 0.65 m from the bottom, that is, at the NCZ–LCZ boundary,
 8 with an injection velocity of 250 L/min. The critical parameter for the fixed level injection process
 9 is the Froude number (Fr), which is a dimensionless number representing the ratio of the kinetic
 10 energy to the gravitational potential energy of the injection fluid. The Froude number can be
 11 calculated using Eq. 4 (Zangrando, 1980):

$$Fr = \left[\frac{(\rho * v^2)}{\Delta\rho * g * B} \right]^{\frac{1}{2}} \quad (4)$$

13 where ρ is the density of the surrounding saline fluid (kg/m^3), v is the injection velocity at the
 14 diffuser outlet (m/s), g is the acceleration due to gravity (m/s^2), $\Delta\rho$ is the density difference
 15 between the injected fluid and the surrounding fluid (kg/m^3), and B is the gap width of the diffuser
 16 (m).

17

18 Experimental experiences (Leblanc et al., 2011; Valderrama et al., 2011) in the establishment of
 19 the gradient show that it is possible to work with a Froude number of approximately 18 or below
 20 to achieve complete mixing at the injection diffuser level and to establish the salinity gradient

1 successfully. In the establishment of the Granada salinity gradient, a value of about 16 near the
2 top of the pond and a value of 4 near the concentrated brine zone are obtained and kept constant
3 along this phase.

4
5 In the injection process, the filling height is split into several layers to ensure the establishment of
6 the expected salinity gradient. Every time the level of water increases by 50 mm, that is, every 1.7
7 hours under a given mass flow rate, the injection process should be stopped for at least 30
8 minutes to reach equilibrium in the layer. Then, a sampling process (as described in Section 2.4)
9 is performed to verify the correct establishment of the salinity gradient, which may take 30
10 minutes more. Therefore, the establishment of each layer requires about 3 hours. Afterwards, the
11 injection process is resumed with the diffusor placed 100 mm higher from the bottom. This
12 process is repeated until the pond water level reaches the NCZ–UCZ boundary, that is, 13
13 injection steps are required during five days. Finally, the solar point design height is reached by
14 injecting fresh water at 25 L/min onto the surface through a floating system to avoid mixing.
15 Figure 5a illustrates the process of establishing the salinity gradient until the pond is filled.
16 Additionally, at the same time as settling the salinity gradient, a temperature gradient is identified
17 in the pond, as can be seen in Figure 5b. The temperature increase reveals both the insulation
18 potential of the salt gradient and the storage capacity of the LCZ even during the filling process.

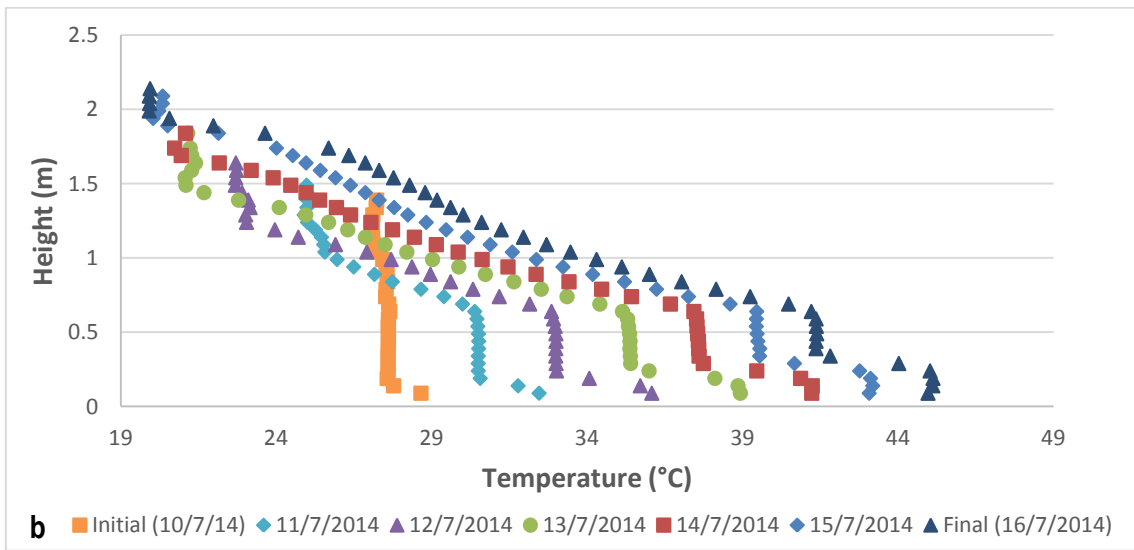
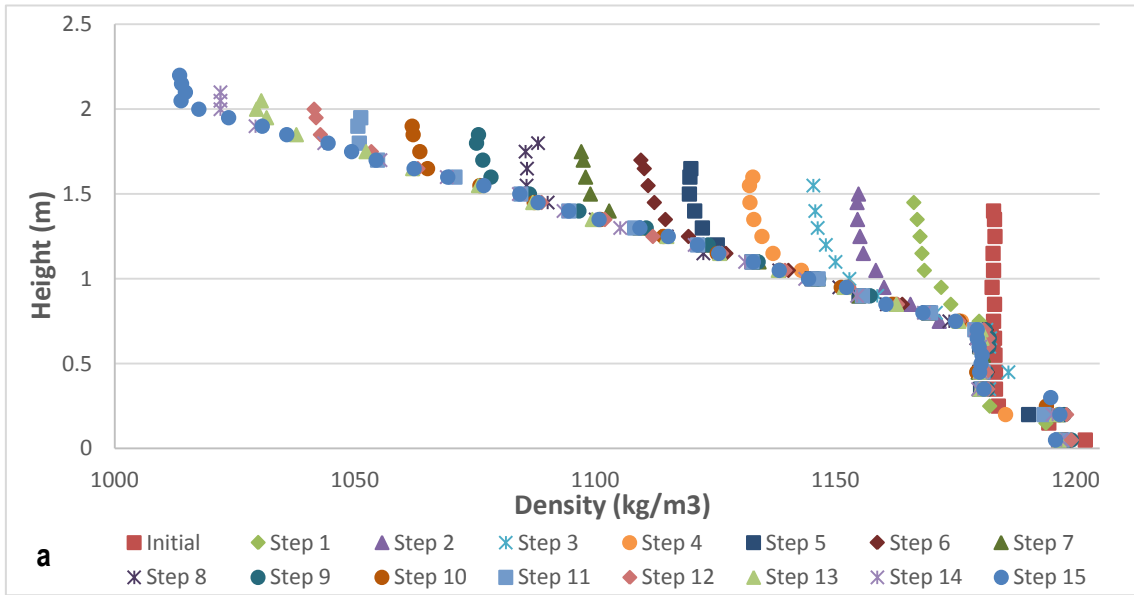


Figure 5. a) Settling of salinity gradient and b) evolution of the temperature gradient during the process of establishing the salinity gradient at the Granada solar pond in July 2014.

3.2 Evolution of salinity gradient

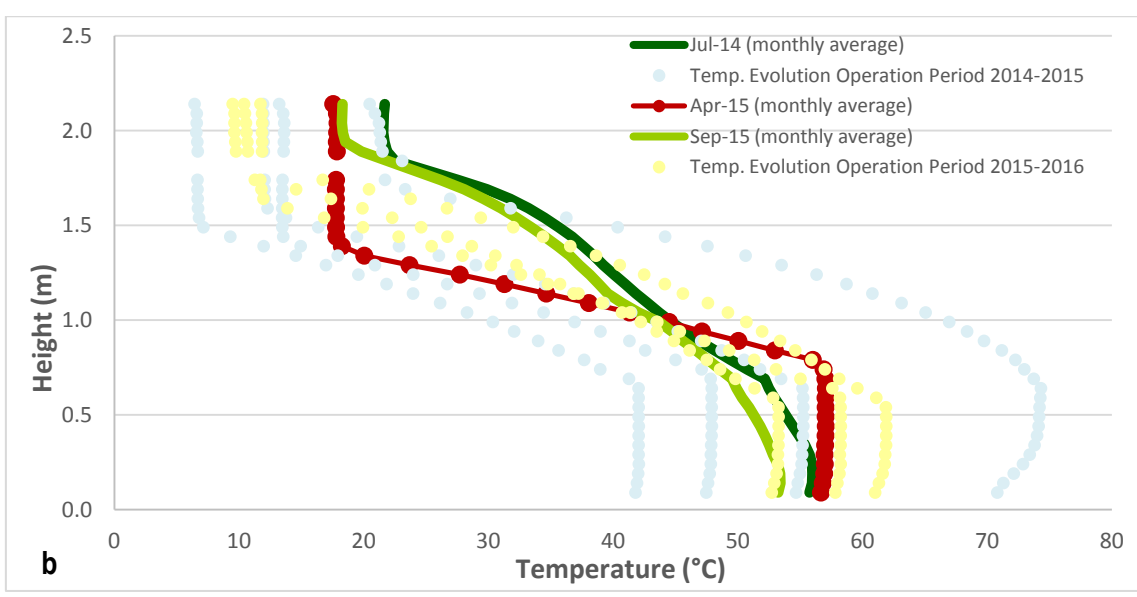
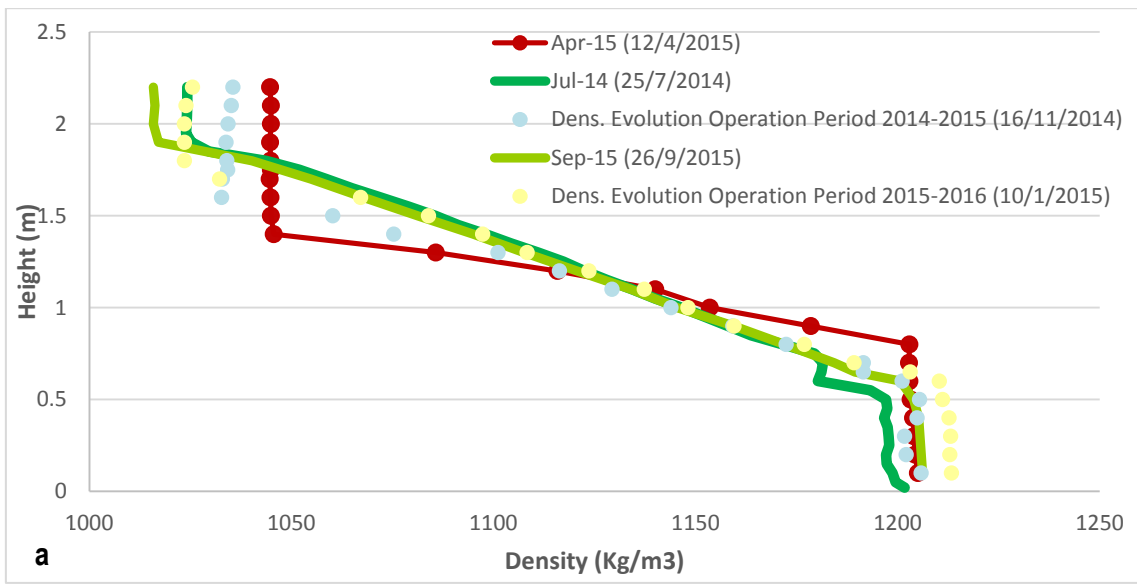
During the operation of the solar pond, different parameters are recorded to control the stability of the system. The salinity gradient (NCZ) is the most critical region in this technology; thus both density and temperature are key parameters to understand the evolution of the gradient.

1 The solar pond in Granada started its operation in July 2014 with the salinity gradient described in
2 Section 3.1 (Figure 5a). In the LCZ, the density was kept almost constant for 10 months with an
3 average value of 1203 kg/m³ and the temperature evolved according to the weather conditions.
4 The initial temperature in the LCZ recorded in the solar pond once the salinity gradient was
5 established was 42.7 °C. Thanks to the high solar radiation during the first month, the
6 temperature in the LCZ increased by 1.5°C per day on average, reaching a maximum
7 temperature of 89 °C at the end of August 2014 (Figure 7). As a result, 63010 MJ was stored in
8 the LCZ alone during the first month of operation.

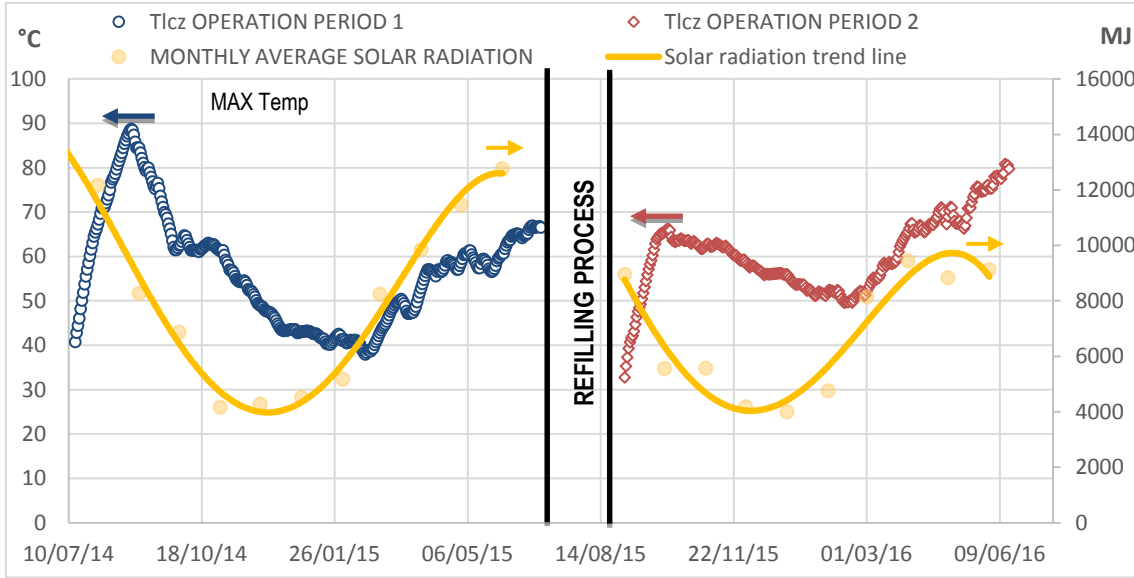
9 As for the UCZ, the density was more variable due to two main aspects: the variations in the
10 ambient air temperature on one hand and the diffusion of the salt from the lower area to the
11 surface on the other. During the operation period, this problem was managed adding fresh water
12 on the surface at a low flow rate. As a result, a maximum surface concentration of 4% was
13 ensured.

14 The degradation of the salinity gradient was detected by the density profile monitoring as the
15 height to the UCZ increases from 0.3 m in July 2014 to 0.8 m in April 2015 (Figure 6a). Although
16 the same trend was observed in the evolution of the temperature profile (Figure 6b), the average
17 monthly temperature of the LCZ not decreased below 40 °C (Figure 7). In April 2015, the salinity
18 gradient was considered to be technically destroyed. Notwithstanding, the system was able to
19 provide the expected heat flow to the flotation unit for two more months, after which the solar
20 pond stopped its operation. During the non-operation period, the system was evaluated based on
21 the recorded data in order to identify the causes of the deterioration of the salinity gradient. As a
22 result, it was concluded that the weather conditions, especially the influence of winds on surface
23 waves, were the main mechanism affecting the stability of the salinity gradient. Additionally, some
24 operation and maintenance patterns would have contributed to the deterioration of the gradient.

1 However, a deeper analysis of the degradation of the salinity gradient is still under evaluation to
 2 predict its appearance and improve the operation and maintenance of the solar pond operation.
 3 In September 2015, the solar pond was refilled using the water injection method as described in
 4 Section 3.1 and its operation was restarted. Figure 6a shows the salinity gradient after the solar
 5 pond was refilled and how it evolved during this second operation period. Degradation of the
 6 salinity gradient was not observed during the second operation period. As for the temperature
 7 evolution, the system was able to keep the LCZ monthly average temperature within a
 8 reasonable range even though the system started working during a clearly less favorable season
 9 (autumn) (Figure 7).



1 Figure 6. a) Evolution of the salinity gradient and b) evolution of the temperature gradient during
 2 operation in 2014 and 2015.



5 Figure 7. Evolution of the LCZ average temperature along the first and second operation periods.

7 The average consumption of salt during the first operation period was 800 kg/month during the
 8 winter season and 1500 kg/month during spring. When the salinity gradient was established, a
 9 large consumption of salt was necessary because the storage area was not at the saturation
 10 concentration. The frequency of the salt supply varied depending on the season. Therefore, the
 11 salt chargers were filled three times a month during the cold months and four or five times per
 12 month during the warm months. As for the fresh water consumed in order to compensate the
 13 losses caused by evaporation and to renovate the surface water, it depends on the weather
 14 conditions and the concentration of salt in the UCZ, which in the case of the Granada solar pond
 15 was set at 4%. The average consumption of low-salinity water was 680 ± 20 m³/year with higher
 16 consumption (>100 m³/month on average) during the summer season (May to September) and
 17 lower consumption during the winter season (December to February) with values below 5
 18 m³/month on average. On the other hand, the clarity of the pond was controlled by the pH, which

1 was maintained at a value of 4, and hydrochloric acid was added when this value increased. The
2 solar pond maintained low values of turbidity and high clarity during these two periods of
3 operation. Solar pond should be monitored and maintained regularly to ensure the conditions for
4 optimal thermal efficiency and rate of heat delivery. Some of the standard maintenance tasks
5 carried out regularly in the Granada solar pond are: i) the density, pH and turbidity profiles of the
6 pond should be monitored once every two weeks and every 10 days during summer season; ii)
7 low salinity water should be added to renovate the surface water only when the concentration of
8 salt in the UCZ is above of 4%; iii) salt chargers should be filled frequently avoiding the need to
9 add large amounts of salt; iv) the temperature profiles can be used as parameters of immediate
10 control of the performance of solar pond and the stability of the boundaries of the gradient zone.

11 12 **3.3 Thermal Efficiency**

13 Thermal efficiency is a key parameter to understand the competitiveness and feasibility of a
14 technology for a specific application. The thermal efficiency of solar ponds is a complex
15 parameter that is highly discussed in the literature. Many authors view solar ponds as a storage
16 technology and consequently define the efficiency as the ratio between the energy stored and the
17 incident solar radiation (Abdullah et al., 2017; Dehghan et al., 2013). Some theoretical models set
18 the energy stored as the total incident radiation minus the heat lost by the system (Bozkurt and
19 Karakilcik, 2015b; Karakilcik et al., 2006). Other authors analyzed the large potential of solar
20 ponds to provide heat to an external system and define the thermal efficiency as the quotient
21 between the heat extracted from the system and the incident solar radiation (Andrews and
22 Akbarzadeh, 2005; Leblanc et al., 2011).

23
24 In all cases, a significant potential of a solar pond is not quantified. The experience of the
25 Granada solar pond proves that the main advantage of a solar pond is the capacity to store

energy in the months with the highest solar radiation to provide a flux of heat to an external system during the whole year. In that context, the thermal efficiency can be expressed as:

$$\eta = \frac{\sum_i Q_{available_i} + \sum_i Q_{extracted_i}}{\sum_i Q_{incident_i}} \quad (5)$$

where $Q_{incident_i}$ is the total incident radiation during day i measured by the temperature sensors, $Q_{extracted_i}$ is the amount of heat extracted from the system during day i and is estimated according to method proposed by Leblanc et al. (Leblanc et al., 2011), and $Q_{available_i}$ represents the part of the solar radiation that the system is capable of storing in the LCZ during day i . On some days, the energy stored in the LCZ may decrease; that is, the system loses its capability to store energy due to unfavorable solar radiation conditions; consequently, $Q_{available_i}$ is assumed to be 0. Thus, $Q_{extracted_i}$ and $Q_{available_i}$ are calculated by Eqs. 6 and 7 as shown below:

$$Q_{extracted_i} = \dot{m} \cdot C_p \cdot (T_{out} - T_{in}) \quad (6)$$

$$Q_{available_i} = \begin{cases} V_{LCZ} \cdot C_p \cdot \rho \cdot (T_{LCZ_i} - T_{LCZ_{i-1}}) & (T_{LCZ_i} - T_{LCZ_{i-1}}) > 0 \\ 0 & (T_{LCZ_i} - T_{LCZ_{i-1}}) < 0 \end{cases} \quad (7)$$

The monthly energy balance in the LCZ is compared to the monthly incident solar radiation (Figure 8). The green area represents the amount of energy stored in the LCZ; the red area represents the energy lost through the walls, bottom, and NCZ; and the blue line represents the amount of energy extracted from the LCZ to supply an external system, in this case, the flotation unit at the mining site. The energy lost in some months is clearly higher than the energy gained; these periods are also the ones with lower incident solar radiation. Notwithstanding, the system is capable of providing a heat flux to the reagent tanks in the flotation unit during the whole year.

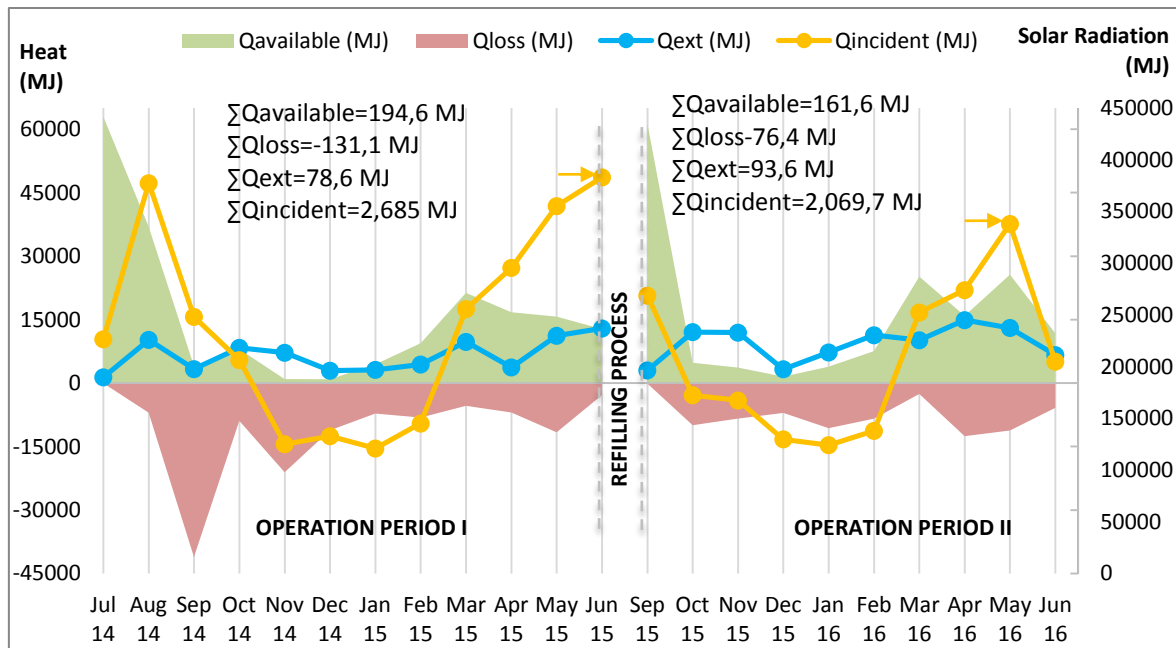


Figure 8. Comparison between energy available, energy losses, energy extracted from the system, and solar radiation (right axis).

As can be seen in Figure 8, identifying a period of operation where the thermal efficiency obtained is representative is a major challenge. The instantaneous method suggested by Date et al. (Date et al., 2013) is a valid model for those systems with a constant heat flux extracted from the pond. Figure 9 shows that the pattern of extraction from the Granada solar pond is significantly variable. Additionally, the large incident solar radiation fluctuations identified during the year may result in large variations in the thermal efficiency obtained from one instant to another; neither periods with the highest radiation nor those with the lowest can be independently considered. In that context, short periods may lead to an unrepresentative estimate of thermal efficiency, and the thermal efficiencies obtained for a monthly balance (Figure 9) confirm this hypothesis. Efficiencies obtained in April 2015, September and December 2014, and December 2015 should be carefully analyzed. Moreover, the thermal efficiency obtained in the first operation month (July 2014) cannot be considered representative since the system has a large capacity to store energy due to the low initial temperature in the pond.

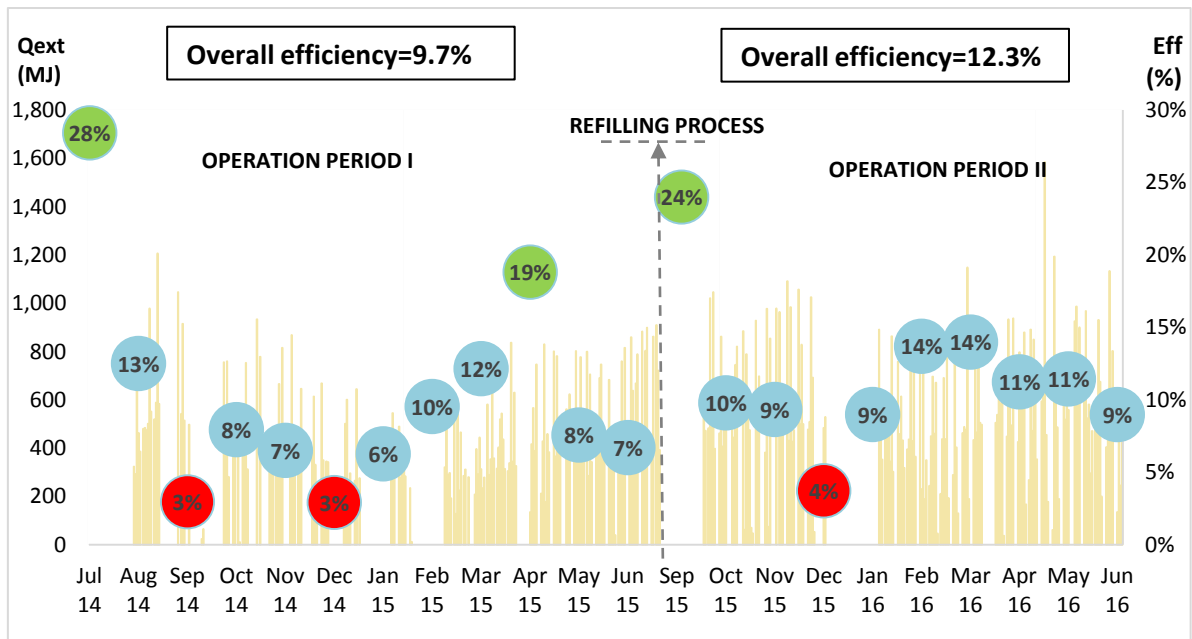


Figure 9. Monthly thermal efficiency and daily extraction rate (bars) of the Granada solar pond.

In that context, a yearly balance is suggested to obtain a reliable value of thermal efficiency and minimize seasonal effects. Overall thermal efficiencies of about 10% are obtained in many experimental studies (Abdullah et al., 2017; Jaefarzadeh, 2004). Through the instantaneous model suggested by Date et al. (Date et al., 2013), an overall efficiency of 17% was obtained for a solar pond in Melbourne. In the Granada solar pond, the overall efficiencies obtained after the first and second operation periods are 9.7 and 12.3%, respectively, with maximum values of 28 and 24% obtained during the first months of operation. The reason of better performance during the second operation period in terms of thermal efficiency is due to the higher amount of heat extracted compared with the first period of operation, as can be seen in Figure 9, the total extraction rate is 19% higher during the second operation period.

It is worth mentioning that the thermal efficiency is a critical parameter that must be evaluated in a long-term perspective and the method proposed in this manuscript attempts to overcome the seasonal (weather) and operational (e.g., amount of heat extracted) effect on the performance of the solar pond.

3.4 Economic and Environmental Savings

The solar pond constructed in Solvay Mineral facilities located in Granada produces part of the low-temperature water required for the mineral purification process, allowing a significant decrease in the amount of fuel oil used by the system. The economic analysis was performed considering the fuel oil bill and the data obtained by monitoring the performance of the solar pond. It is worth mentioning that operational expenses depend on the amount of fuel consumed and the volatile fossil fuel market.

In the years before the construction of the solar pond (2011–2013), the amount of fuel consumed per year by the flotation unit ranged between 22700 and 25330 L with an average hourly consumption of 5.2 L/h. The extractions from the solar pond saved 11060 L and 7845 L of fuel oil during the first and second periods of operation. Therefore, the hourly average consumption decreased to 2.9 and 3.2 L/h, resulting in reductions of 44 and 38% in the amount of fuel oil burned during each operation period. Additionally, during the initial six months of the first operation period, the average consumption achieved a minimum value of 1.67 L/h, reducing the fuel oil consumption by almost 68%. Regarding the economic savings, the cost (fuel oil bill) was reduced by a higher percentage than the consumption of fuel oil, due to the decreasing trend of the fuel oil prices during 2014 and 2015, amounting to reductions of 52 and 68% in the first and second periods of operation, respectively, compared to the 2013.

The destruction of the salinity gradient altered the operation of the solar pond, which caused two months of inactivity, July and August 2015. Along this two months all heat required by the flotation unit was supplied by the boiler. Consequently, the consumption of fuel oil increased from 1.36L/h in 2014 to 2.64 L/h in 2015. Despite the increase in terms of hourly consumption, the flotation unit reduced its operation by almost half, from 433 h/month to 226 h/month on average. As a result, the extra fuel burned due to the inoperability of the solar pond had an estimated cost of 350 €. However, the most significant penalty cost associated with the deterioration of the

1 salinity gradient was due to the emptying of the pond and to restore the salinity gradient, which
2 can be estimated at 8000 €.

3 In addition, not only did the solar pond reduce the operating costs considerably, but also the
4 environmental costs were clearly reduced. The emission factor of the fuel oil consumed in Spain
5 is estimated to be 2.868 kg CO₂/L (OECC, 2017); consequently, 31.7 and 22.5 tons of CO₂
6 emissions were avoided during the first and second periods of operation due to the use of the
7 solar pond system.

8
9 **4. Conclusions**

10 In this study, a square industrial solar pond designed, constructed, and operated during two
11 periods (2014–2015) at the mining facilities of Solvay Minerales in Granada (Spain) is presented.

12 The purpose of this solar pond is to preheat the process water and the reagents at the flotation
13 unit of the mining facility.

14 The establishment of the salinity gradient was successful performed by the water injection
15 method using a Froude number of 16 near the top of the pond and a value of 4 near the
16 concentrated brine zone. A degradation of the salinity gradient was detected by the density profile
17 monitoring, and salinity gradient was considered to be technically destroyed in April 2015. The
18 analysis of the monitoring data concluded that the weather conditions, especially the influence of
19 winds on surface waves, were the main mechanism affecting the stability of the salinity gradient.
20 Additionally, some operation and maintenance patterns would have contributed to the
21 deterioration of the gradient. It is worth to mention, the system was able to provide the expected
22 heat flow to the flotation unit for two more months, after which the solar pond stopped its
23 operation.

24 The experience of the Granada solar pond proves that the main advantage of a solar pond is the
25 capacity to store energy in the months with the highest solar radiation to provide a flux of heat to

1 an external system during the whole year. In terms of energy efficiency, a yearly balance is
2 suggested to obtain a reliable value of thermal efficiency and minimize seasonal effects. The
3 overall efficiencies obtained after the first and second operation periods are 9.7 and 12.3%,
4 respectively, with maximum values of 28 and 24% obtained during the first months of operation.
5 The fuel oil cost was reduced by a higher percentage than the fuel oil consumption, due to the
6 decreasing tendency of the fuel oil prices during 2014 and 2015. In terms of the environmental
7 costs, greenhouse gas emission reductions amounting to 31.7 and 22.5 t of CO₂ were avoided
8 during the first and second periods of operation due to the heat supplied by the Granada solar
9 pond system.

10 A recommendation for future work is to perform a deeper analysis on the destruction of the
11 salinity gradient reported in this manuscript, this phenomenon has hardly been discussed or
12 reported in the literature and it should be considered of great importance to elucidate the
13 mechanisms that cause this degradation and also formulate maintenance actions that can avoid
14 it.

16 **Acknowledgments**

17 The authors gratefully acknowledge personnel from Solvay Minerales facilities for practical
18 assistance, especially to M. Gonzalez and C. Gonzalez for their valuable cooperation. This
19 research was financially supported by the Ministry of Science and Innovation (MICINN, Spain)
20 WASTE2PRODUCT project and the Catalan Government (Project Ref. 2014SGR050).

22 **5. References**

23 Abdullah, A.A., Fallatah, H.M., Lindsay, K.A., Oreijah, M.M., 2017. Measurements of the
24 performance of the experimental salt-gradient solar pond at Makkah one year after
25 commissioning. Sol. Energy 150, 212–219. doi:10.1016/j.solener.2017.04.040

1
2
3
4
5
6
7
8
9
10
11
12
13
14
15
16
17
18
19
20
21
22
23
24
25
26
27
28
29
30
31
32
33
34
35
36
37
38
39
40
41
42
43
44
45
46
47
48
49
50
51
52
53
54
55
56
57
58
59
60
61
62
63
64
65

1 Alcaraz, A., Valderrama, C., Cortina, J. L., Akbarzadeh, A., Farran A., 2016. Enhancing the
2 efficiency of solar pond heat extraction by using both lateral and bottom heat exchangers.
3 Solar Energy 134, 82-94.
4 Akbarzadeh, A., Manins, P., 1988. Convective layers generated by side walls in solar ponds. Sol.
5 Energy 41, 521–529.
6 Andrews, J., Akbarzadeh, A., 2005. Enhancing the thermal efficiency of solar ponds by extracting
7 heat from the gradient layer. Sol. Energy 78, 704–716. doi:10.1016/j.solener.2004.09.012
8 Bernad, F., Casas, S., Gibert, O., Akbarzadeh, A., Cortina, J.L., Valderrama, C., 2013. Salinity
9 gradient solar pond: Validation and simulation model. Sol. Energy 98, 366–374.
10 doi:10.1016/j.solener.2013.10.004
11 Bozkurt, I., Karakilcik, M., 2015a. The effect of sunny area ratios on the thermal performance of
12 solar ponds. Energy Conversion and Management 91, 323-332.
13 Bozkurt, I., Karakilcik, M., 2015b. Exergy analysis of a solar pond integrated with solar collector.
14 Sol. Energy 112, 282–289. doi:10.1016/j.solener.2014.12.009
15 Bryant, R.S., Bowser, R.P., Wittenberg, L.J., 1979. Construction and initial operation of the
16 Miaisburg salt-gradient solar pond. Electr. Power Res. Inst. EPRI EA 1005–1009.
17 Collins, R.B., 1984. Alice Spring solar pond project. Pergamon Press, Oxford, Engl, Perth, Aust,
18 pp. 775–779.
19 Date, A., Yaakob, Y., Date, A., Krishnapillai, S., Akbarzadeh, A., 2013. Heat extraction from Non-
20 Convective and Lower Convective Zones of the solar pond: A transient study. Sol. Energy
21 97, 517–528. doi:10.1016/j.solener.2013.09.013
22 Davey, T.R.A., 1968. The aspendaley solar pond. Rep. R15.
23 Dehghan, A.A., Movahedi, A., Mazidi, M., 2013. Experimental investigation of energy and exergy
24 performance of square and circular solar ponds. Sol. Energy 97, 273–284.
25 doi:10.1016/j.solener.2013.08.013

1
2
3
4
5
6
7
8
9
10
11
12
13
14
15
16
17
18
19
20
21
22
23
24
25
26
27
28
29
30
31
32
33
34
35
36
37
38
39
40
41
42
43
44
45
46
47
48
49
50
51
52
53
54
55
56
57
58
59
60
61
62
63
64
65

1 Ding, L.C., Akbarzadeh, A., Date, A., 2016. Transient model to predict the performance of
2 thermoelectric generators coupled with solar pond. *Energy* 103, 271–289.
3 doi:10.1016/j.energy.2016.02.124
4
5 Ding, L.C., Akbarzadeh, A., Date, A., Frawley, D.J., 2016. Passive small scale electric power
6 generation using thermoelectric cells in solar pond. *Energy* 117, 149–165.
7 doi:10.1016/j.energy.2016.10.085
8
9 Folchitto, S., 1997. Experience with a solar pond at Margherita di Savoia, in: Claridge D.E., P.J.E.
10 (Ed.), *International Solar Energy Conference*. ASME, New York, NY, United States,
11 Washington, DC, USA, pp. 223–228.
12
13 Fynn, R.P., 1981. A solar pond-assisted heat pump for greenhouses 26, 491–496.
14
15 Ganguly, S., Jain, R., Date, A., Akbarzadeh, A., 2017. On the addition of heat to solar pond from
16 external sources. *Solar Energy* 144, 111-116.
17
18 Golding, P., Akbarzadah, A., Davey, J.A., McDonald, P.W.G., Charter, W.W.S., 1982. Design
19 features and construction of Laverton solar ponds, I.S.E.S.A.N.Z. Sect. Conf.
20
21 Hull, J.R., Bushnell, D.L., Sempsrote, D.G., Pena, A., 1989. Ammonium sulfate solar pond: Obser
22 vations from small-scale experiments. *Sol. Energy* 43, 57–64. doi:10.1016/0038-
23 092X(89)90100-X
24
25 Hull, J.R., Nielsen, C.E., 1988. Steady state analysis of the rising solar pond, *Solar Energy*
26 *Technology*. Proc. ASME 1508–1512.
27
28 Jaefarzadeh, M.R., 2004. Thermal behavior of a small salinity-gradient solar pond with wall
29 shading effect. *Sol. Energy* 77, 281–290. doi:10.1016/j.solener.2004.05.013
30
31 Karakilcik, M., Dincer, I., Rosen, M.A., 2006. Performance investigation of a solar pond. *Appl.*
32 *Therm. Eng.* 26, 727–735. doi:10.1016/j.applthermaleng.2005.09.003
33
34 Khalilian, M., 2017a. Assessment of the overall energy and exergy efficiencies of the salinity
35 gradient solar pond with shading effect. *Solar Energy* 158, 311-320

1
2
3
4
5
6
7
8
9
10
11
12
13
14
15
16
17
18
19
20
21
22
23
24
25
26
27
28
29
30
31
32
33
34
35
36
37
38
39
40
41
42
43
44
45
46
47
48
49
50
51
52
53
54
55
56
57
58
59
60
61
62
63
64
65

1 Khalilian, M., 2017b. Exergetic performance analysis of a salinity gradient solar pond. Solar
2 Energy 157, 895-904.

3 Kumar, A., Kishore, V.V.N., 1999. Construction and operational experience of a 6000 M2 solar
4 pond at kutch, India. Sol. Energy 65, 237–249. doi:10.1016/S0038-092X(98)00134-0

5 Leblanc, J., Akbarzadeh, A., Andrews, J., Lu, H., Golding, P., 2011. Heat extraction methods from
6 salinity-gradient solar ponds and introduction of a novel system of heat extraction for
7 improved efficiency. Sol. Energy. doi:10.1016/j.solener.2010.06.005

8 Lesino, G., Saravia, L., Galli, D., 1990. Industrial production of sodium sulfate using solar
9 ponds. Sol. Energy 45, 215–219.

10 Lesino, G., Saravia, L., 1991. Solar ponds in hydrometallurgy and salt production. Sol. Energy 46,
11 377–382.

12 Liao, Y., Swift, A. & Golding, P., 1988. Determination of the critical Froude number for gradient
13 establishment in a solar pond. Sol. Eng. 101–105.

14 Mehta, A.S., Pathak, N., Shah, B.M., Gomkale, S.D., 1988. Performance analysis of a bittern-
15 based solar pond. Sol. Energy 40, 469–475.

16 Newell, T.A., Cowie, R.G., Upper, J.M., Smith, M.K., Cler, G.L., 1990. Construction and operation
17 activities at the University of Illinois Salt Gradient Solar Pond. Sol. Energy 45, 231–239.
18 doi:10.1016/0038-092X(90)90091-P

19 Nie, Z., Bu, L., Zheng, M., Huang, W., 2011. Experimental study of natural brine solar ponds in
20 Tibet. Sol. Energy 85, 1537–1542. doi:10.1016/j.solener.2011.04.011

21 Nielsen, C.E., 1980. No Title. Sol. Energy Technol. Handb.

22 Njokua, H. O., Agashia, B. E., Onyegegbu, S. O., 2017. A numerical study to predict the energy
23 and exergy performances of a salinity gradient solar pond with thermal extraction. Solar
24 Energy 15, 744-761.

1
2
3
4
5
6
7
8
9
10
11
12
13
14
15
16
17
18
19
20
21
22
23
24
25
26
27
28
29
30
31
32
33
34
35
36
37
38
39
40
41
42
43
44
45
46
47
48
49
50
51
52
53
54
55
56
57
58
59
60
61
62
63
64
65

1 OECC, 2017. Factores de Emisión. Registro de la huella de carbono, compensacion y proyectos
2 de absorción de dióxido de carbono. s.l.: Ministerio de Agricultura y Pesca, Alimentación y
3 Medio Ambiente.
4 Patel, S.M., Gupta, C.L., 1981. Experimental solar pond in a hot humid climate. Sunworld 5, 115–
5 118.
6 Rabl, A., Nielsen, C.E., 1975. Solar ponds for space heating. Sol. Energy 17, 1–12.
7 Rahaoui, K., Ding, L .C., Tan, L. P., Mediouri, W., Mahmoudi, F., Nakoa, K., Akbarzadeh, A.,
8 2017. Sustainable membrane distillation coupled with solar pond. Energy Procedia 110, 414
9 – 419.
10 Reid, R.L., MeLean, T.J., Lai, C.-H., 1985. Feasibility study of a solar pond/IPH/electrical supply
11 for a food canning plant, in: Solar Engineering. pp. 263–270.
12 Sayer, A. H., Monjezi, A. A., Campbell, A. N., 2018. Behaviour of a salinity gradient solar pond
13 during two years and the impact of zonal thickness variation on its performance. Applied
14 Thermal Engineering 130, 1191–1198.
15 Shah, S.A., Short, T.H., Fynn, R.P., 1981. Modeling and testing a salt gradient solar pond in
16 northeast Ohio. Sol. Energy 27, 393–401.
17 Sherman, B.S., Imberger, J., 1991. Control of a solar pond. Sol. Energy 46, 71–81.
18 doi:10.1016/0038-092X(91)90018-R
19 Simic, M., George, J., 2017. Design of a system to monitor and control solar pond: A review.
20 Energy Procedia 110, 322 – 327.
21 Srinivasan, J., 1993. Solar pond technology 18, 39–55.
22 Srinivasan, J., 1990. Performance of a small solar pond in the tropics. Sol. Energy 45, 221–230.
23 Swift, A.H.P., Reid, R.L., Sewell, M.P., Boegli, W.J., 1987. Operation results for a 3355 m2 solar
24 pond in El Paso, Texas., in: Solar Engineering. pp. 287–293.

1
2
3
4
5
6
7
8
9
10
11
12
13
14
15
16
17
18
19
20
21
22
23
24
25
26
27
28
29
30
31
32
33
34
35
36
37
38
39
40
41
42
43
44
45
46
47
48
49
50
51
52
53
54
55
56
57
58
59
60
61
62
63
64
65

1 Tabor, H., Doron, B., 1986. Solar Ponds-lesson learned from the 150 K We power plant at Ein
2 Boqek. Proc. ASME Sol. Energy Div.
3 Tabor, H.Z., Doron, B., 1990. The Beith Ha'Arava 5 MW(e) Solar Pond Power Plant (SPPP)-
4 Progress report. Sol. Energy 45, 247–253. doi:10.1016/0038-092X(90)90093-R
5 Torkmahalleh, M. A., Askari, M., Gorjinezhad, S., Erog, D., Obaidullah, M., Habib, A. R., Godelek,
6 S., et al., 2017. Key factors impacting performance of a salinity gradient solar pond exposed
7 to Mediterranean climate. Solar Energy 15, 321-329.
8 Valderrama, C., Gibert, O., Arcal, J., Solano, P., Akbarzadeh, A., Larrotcha, E., Cortina, J.L.,
9 2011. Solar energy storage by salinity gradient solar pond: Pilot plant construction and
10 gradient control. Desalination 279, 445–450. doi:10.1016/j.desal.2011.06.035
11 Valderrama, C., Luis Cortina, J., Akbarzadeh, A., 2016. Solar Ponds, in: Storing Energy: With
12 Special Reference to Renewable Energy Sources. pp. 273–289. doi:10.1016/B978-0-12-
13 803440-8.00014-2
14 Wilkins, E., Lee, T.K., Chakraborti, S., 1986. Optimization of the gel solar pond parameters:
15 Comparison of analytical models. Energy Convers. Manag. 26, 123–134.
16 Yu, N., Wang, R.Z., Wang, L.W., 2013. Sorption thermal storage for solar energy. Prog. Energy
17 Combust. Sci. 39, 489–514. doi:10.1016/j.pecs.2013.05.004
18 Zangrando, F., 1980. A simple method to establish salt gradient solar ponds. Sol. Energy 25,
19 467–470. doi:10.1016/0038-092X(80)90456-9
20 Zangrando, F., 1991. On the hydrodynamics of salt-gradient solar ponds. Sol. Energy 46, 323–
21 341.
22 Zhang, G., Wu, Z., Cheng, F., Min, Z., Lee, D. J., 2016. Thermophilic digestion of waste-activated
23 sludge coupled with solar pond. Renewable Energy 98,142-147.